Recents Results of Global Convective Dynamo Simulations

Jörn Warnecke

Max Planck Institute
for Solar System Research

Axel Brandenburg, Nordita
Petri J. Käpylä, Helsinki University
Maarit J. Käpylä, Aalto University

Solar Cycle

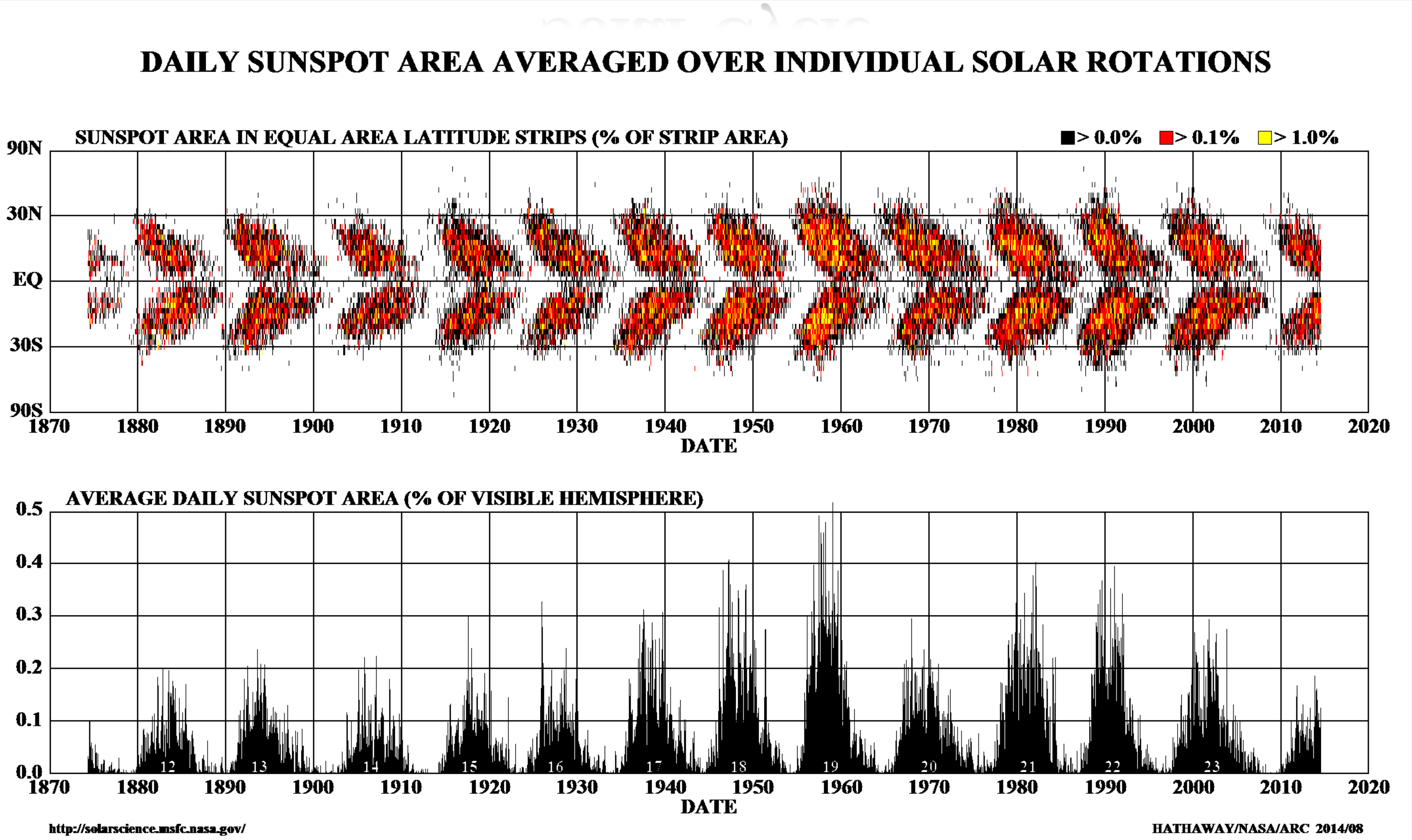

DAILY SUNSPOT AREA AVERAGED OVER INDIVIDUAL SOLAR ROTATIONS
SUNSPOT AREA IN EQUAL AREA LATITUDE STRIPS (% OF STRIP AREA)
> 0.0%
> 0.1%
> 1.0%
90N
30N
EQ
30S
90S
1870
1880
1890
1900
1910
1920
1930
1940
1950
1960
1970
1980
1990
2000
2010
2020
DATE
AVERAGE DAILY SUNSPOT AREA (% OF VISIBLE HEMISPHERE)
0.5
0.4
0.3
0.2
0.1
0.0
12
13
14
15
16
17
18
19
20
21
22
23
http://solarscience.msfc.nasa.gov/
HATHAWAY/NASA/ARC 2014/08

Solar Cycle

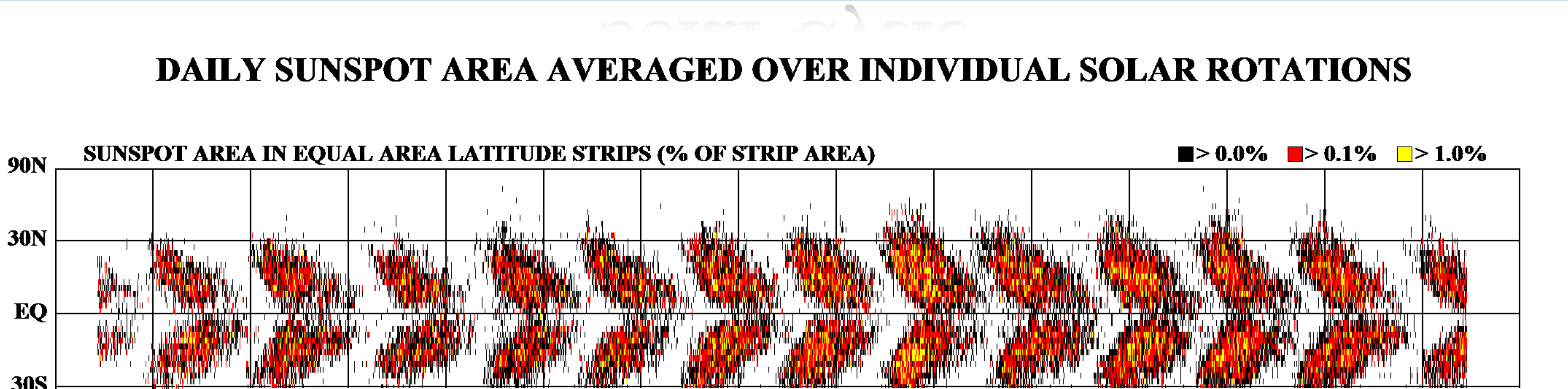

DAILY SUNSPOT AREA AVERAGED OVER INDIVIDUAL SOLAR ROTATIONS
SUNSPOT AREA IN EQUAL AREA LATITUDE STRIPS (% OF STRIP AREA)
> 0.0%
> 0.1%
> 1.0%
90N
30N
EQ
30S
90S
1870
1880
AVERAGE D
0.5
0.4
0.3
0.2
0.1
0.0
12
http://solarscience.msf

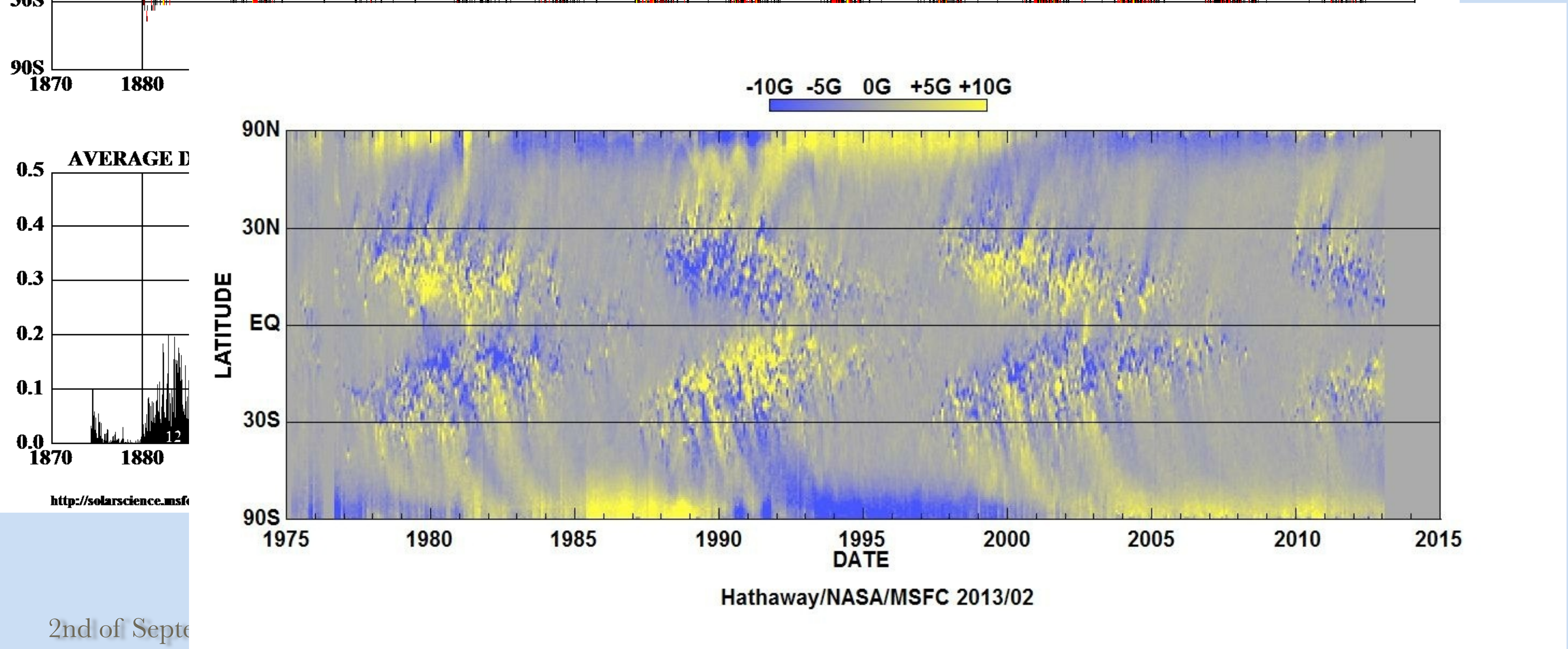

-10G -5G 0G +5G +10G
90N
30N
EQ
30S
90S
LATITUDE
1975
1980
1985
1990
1995
2000
2005
2010
2015
DATE
Hathaway/NASA/MSFC 2013/02

Solar Cycle

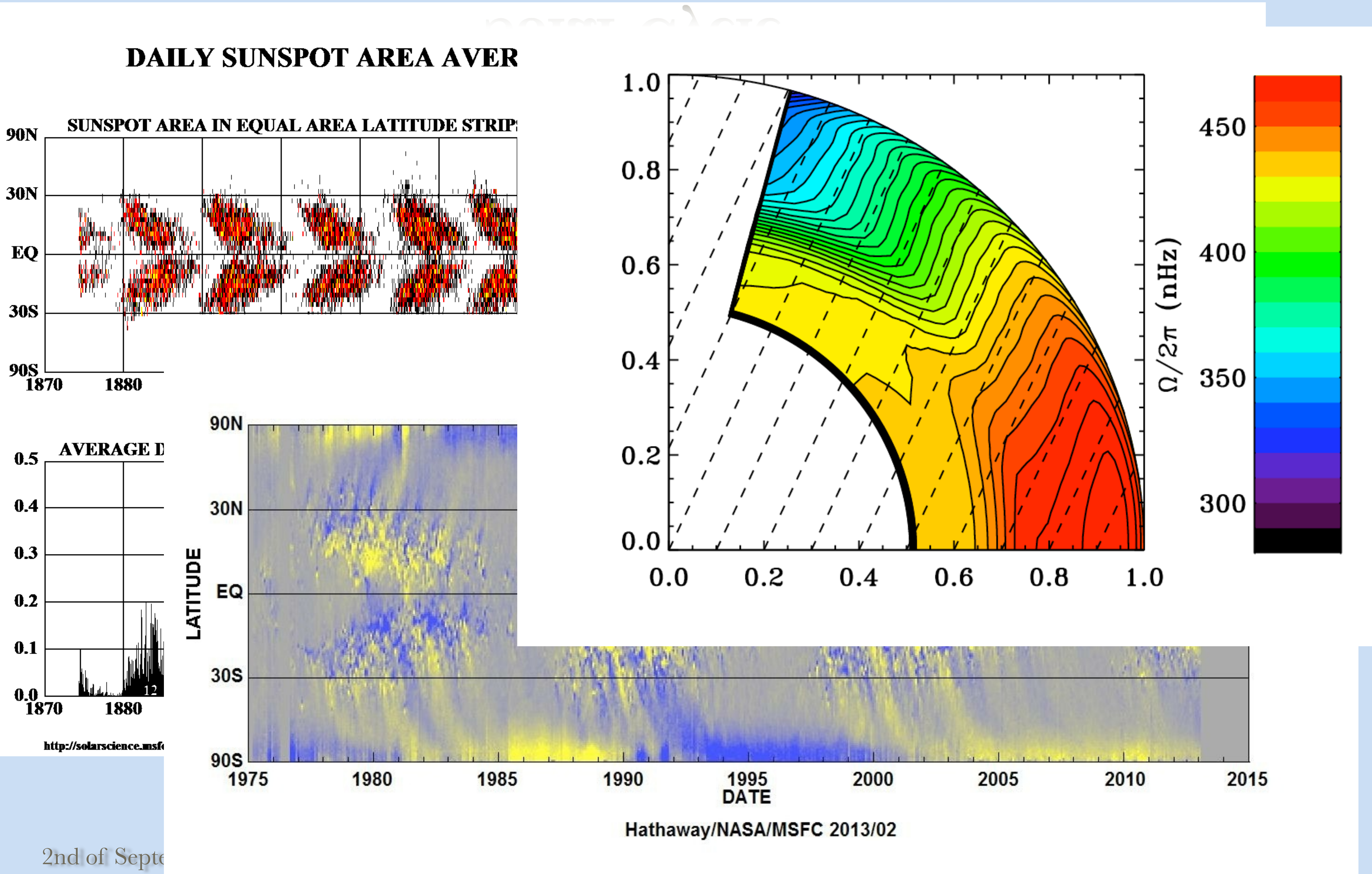
DAILY SUNSPOT AREA AVER
SUNSPOT AREA IN EQUAL AREA LATITUDE STRIP
90N
30N
EQ
30S
90S
1870
1880
AVERAGE D
0.5
0.4
0.3
0.2
0.1
0.0
1870
1880
http://solarscience.msf
90N
30N
EQ
30S
90S
LATITUDE
1975
1980
1985
1990
1995
2000
2005
2010
2015
DATE
Hathaway/NASA/MSFC 2013/02
1.0
0.8
0.6
0.4
0.2
0.0
0.0
0.2
0.4
0.6
0.8
1.0
Ω/2π (nHz)
450
400
350
300

Global convective dynamo simulations

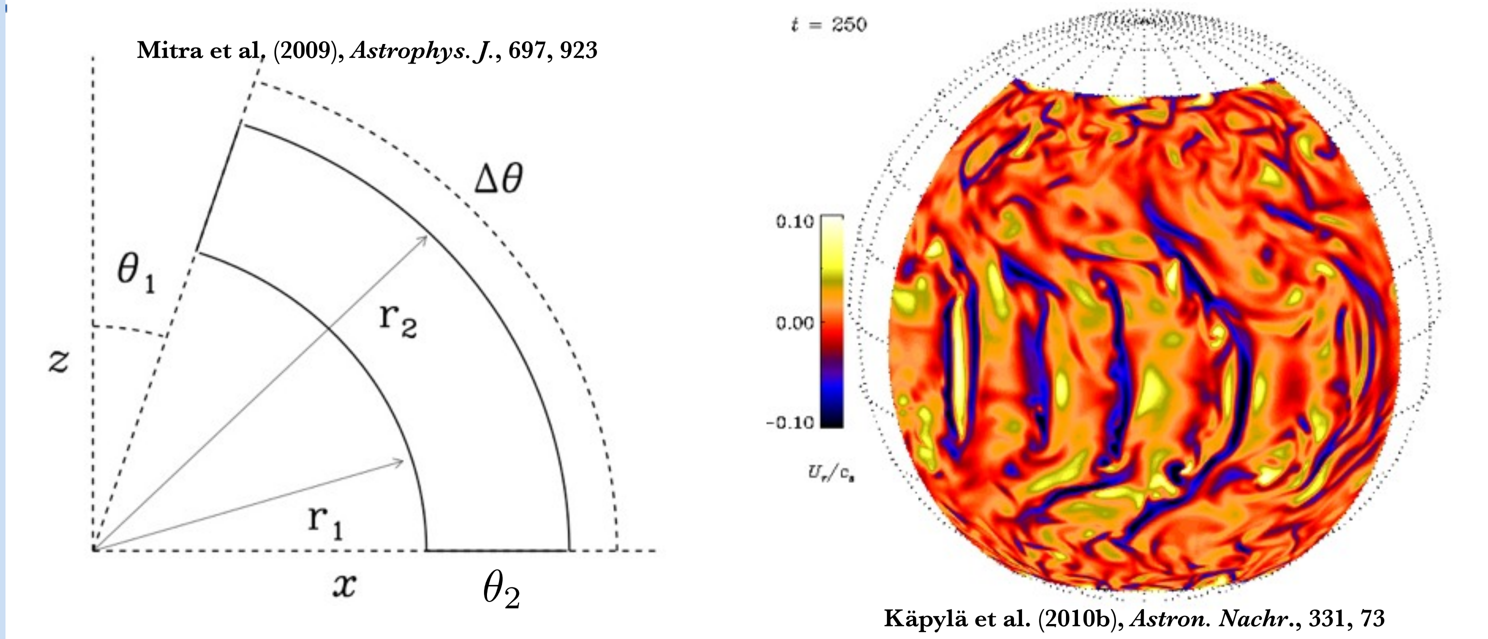

- high-order finite-difference code
- scales up efficiently to over 60.000 cores
- compressible MHD

$0.7R < r < R \qquad \theta_1 < \theta < \theta_2 \qquad 0 < \phi < \Delta\phi \qquad k_\mathrm{f} = 2\pi/\Delta R$

We model a spherical sector (`wedge') where only parts of the latitudinal and longitudinal extents are taken into account.

Normal field condition for *B* at the outer radial boundary and perfect conductor at all other boundaries. Impenetrable stress-free boundaries on all boundaries.

Equatorward Migration

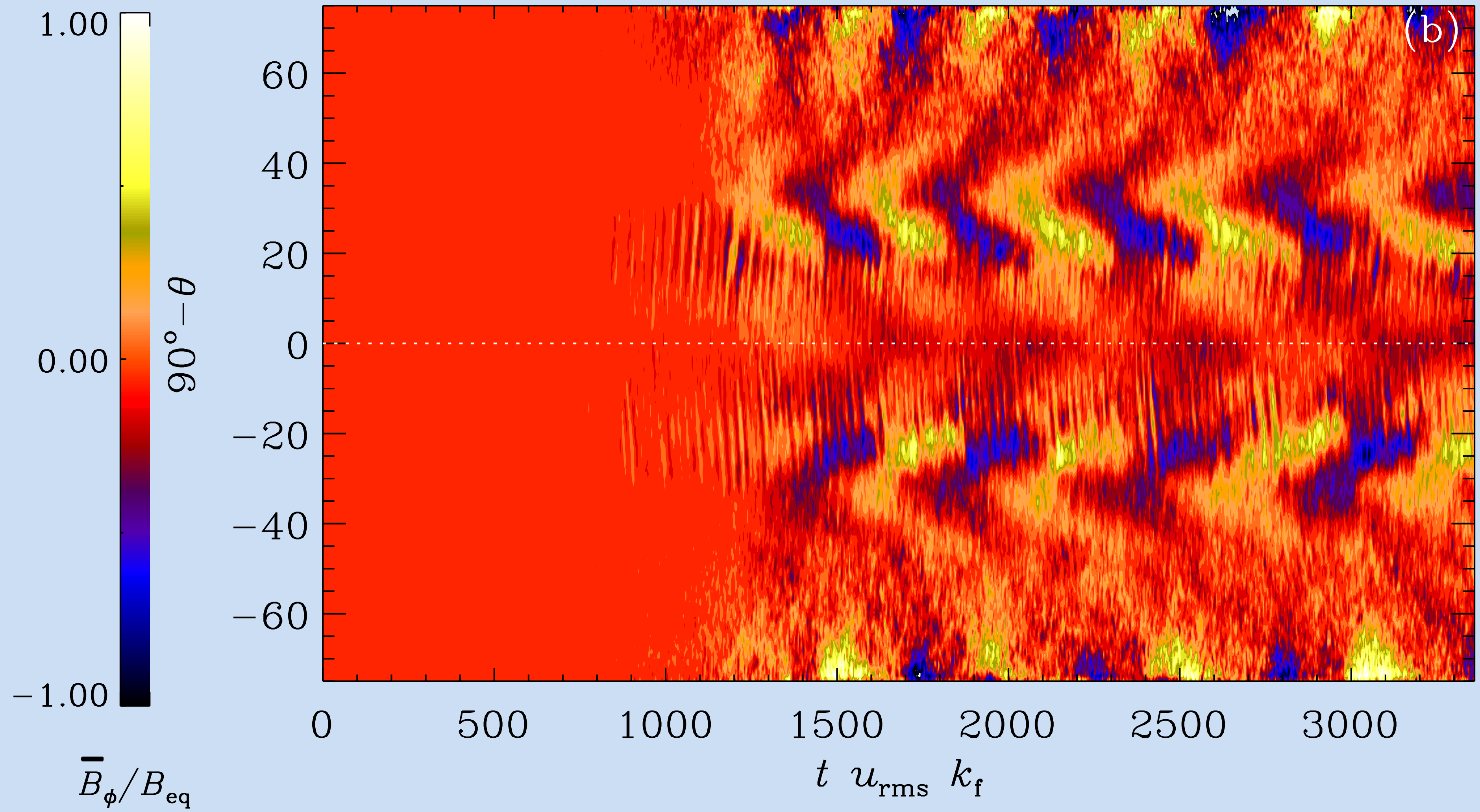

Käpylä, Mantere & Brandenburg 2012 (ApJL 755, L22)

Equatorward Migration

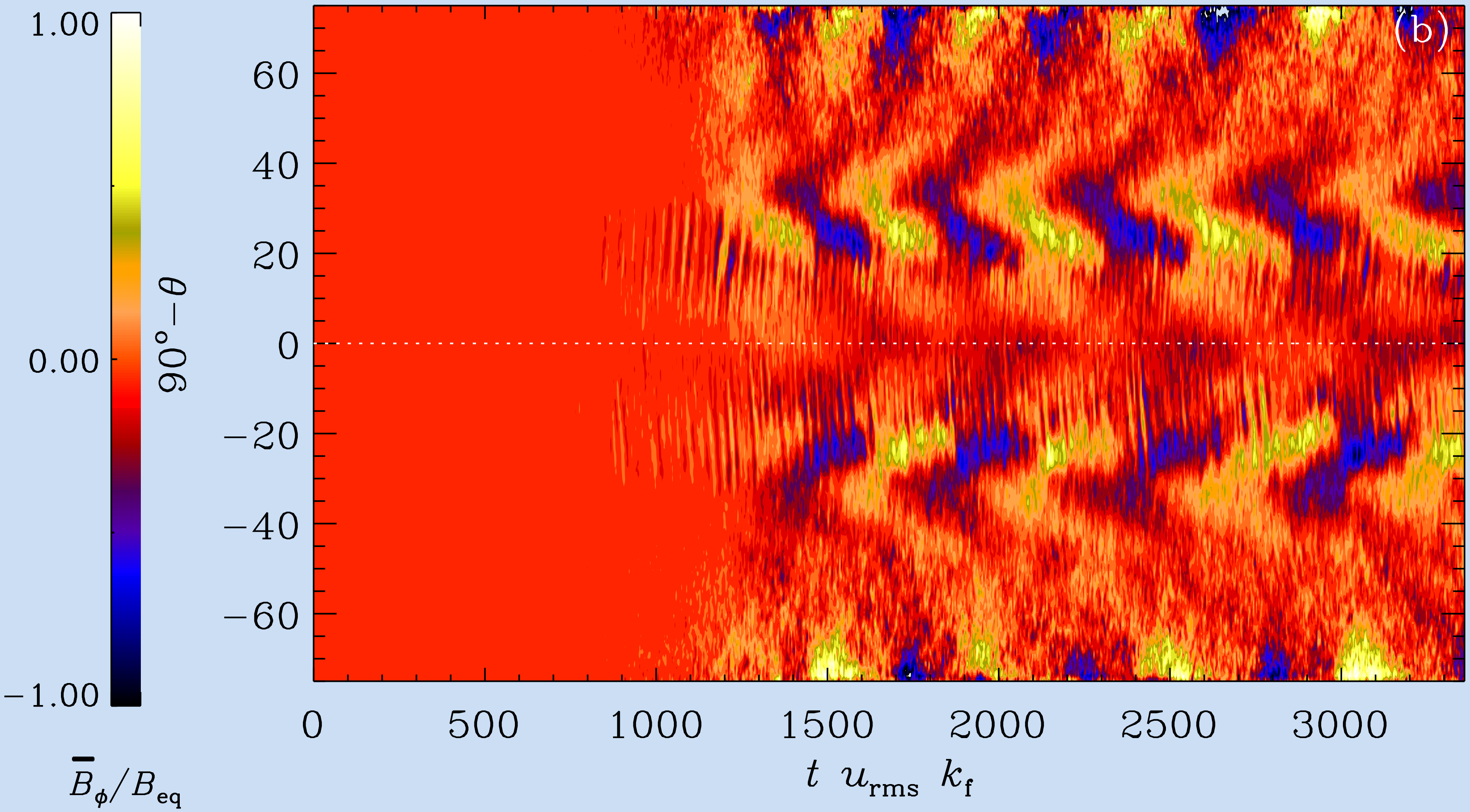

Käpylä, Mantere & Brandenburg 2012 (ApJL 755, L22)

Equatorward Migration

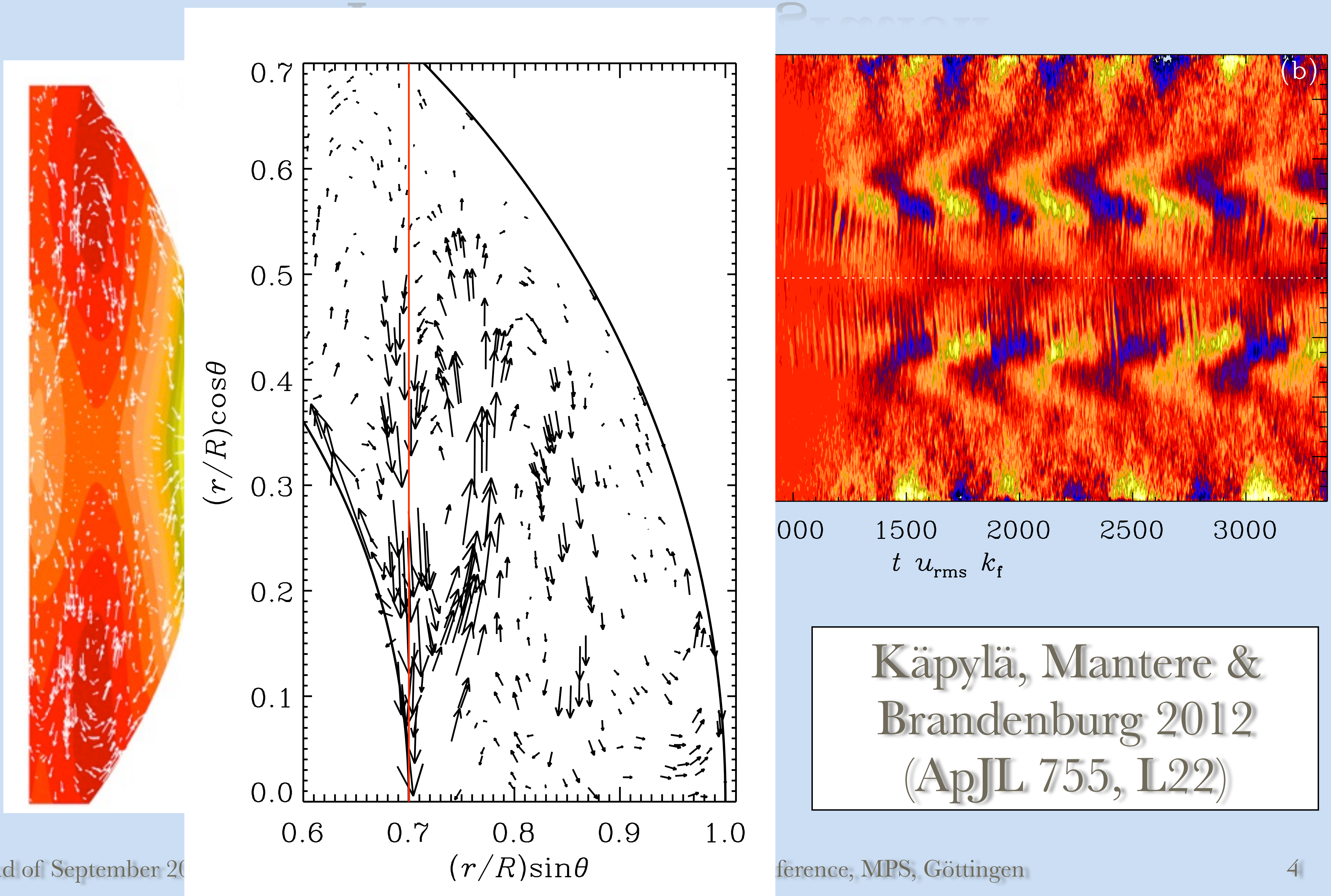

Käpylä, Mantere & Brandenburg 2012 (ApJL 755, L22)

Cause of Equatorward Migration

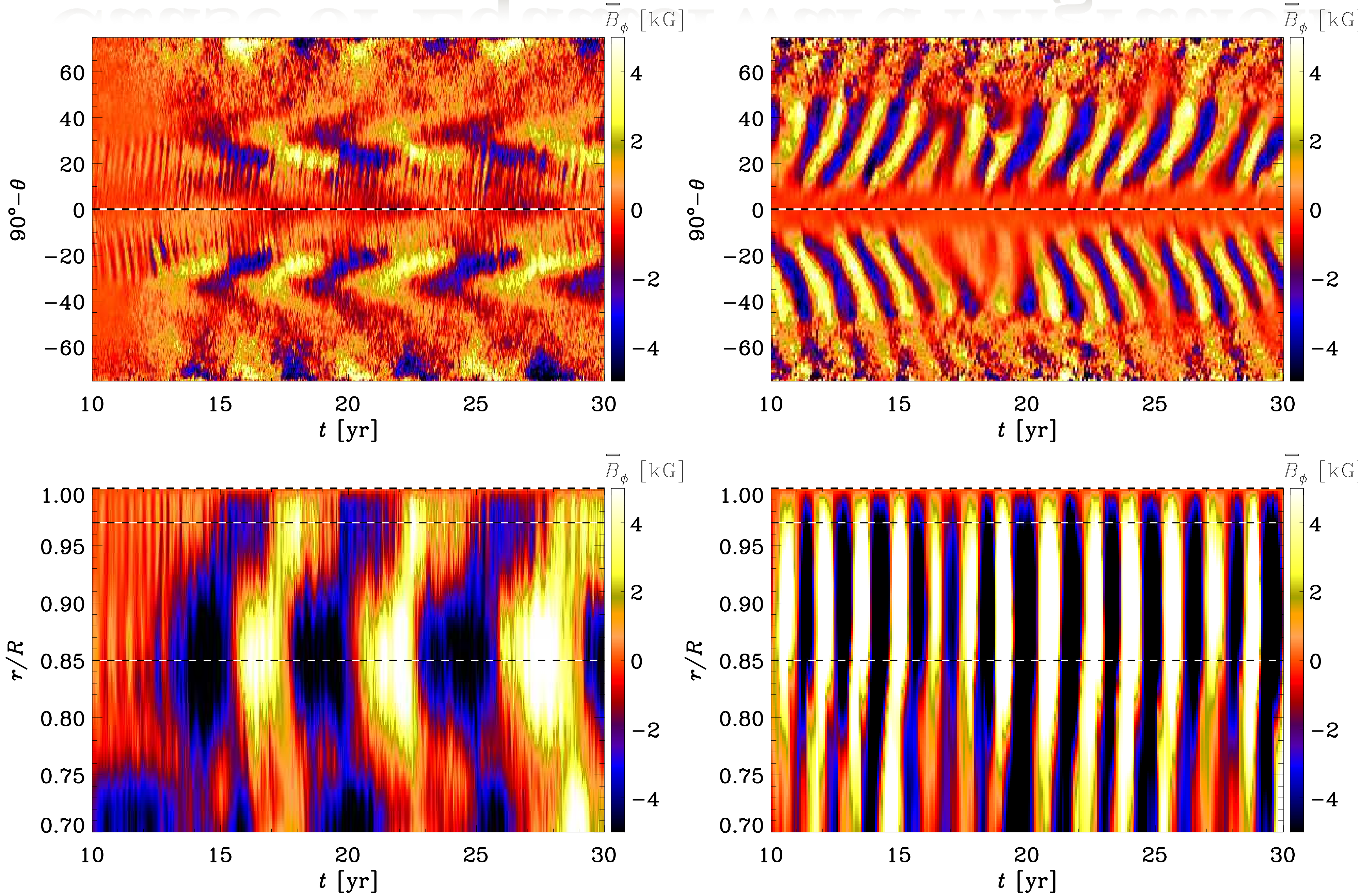

$\mathrm{Pr}=\nu/\chi=2.5$

$\mathrm{Pm}=\nu/\eta=1$

$\mathrm{Pr}=0.5$

$\mathrm{Pm}=0.5$

Parker—Yoshimura—Rule

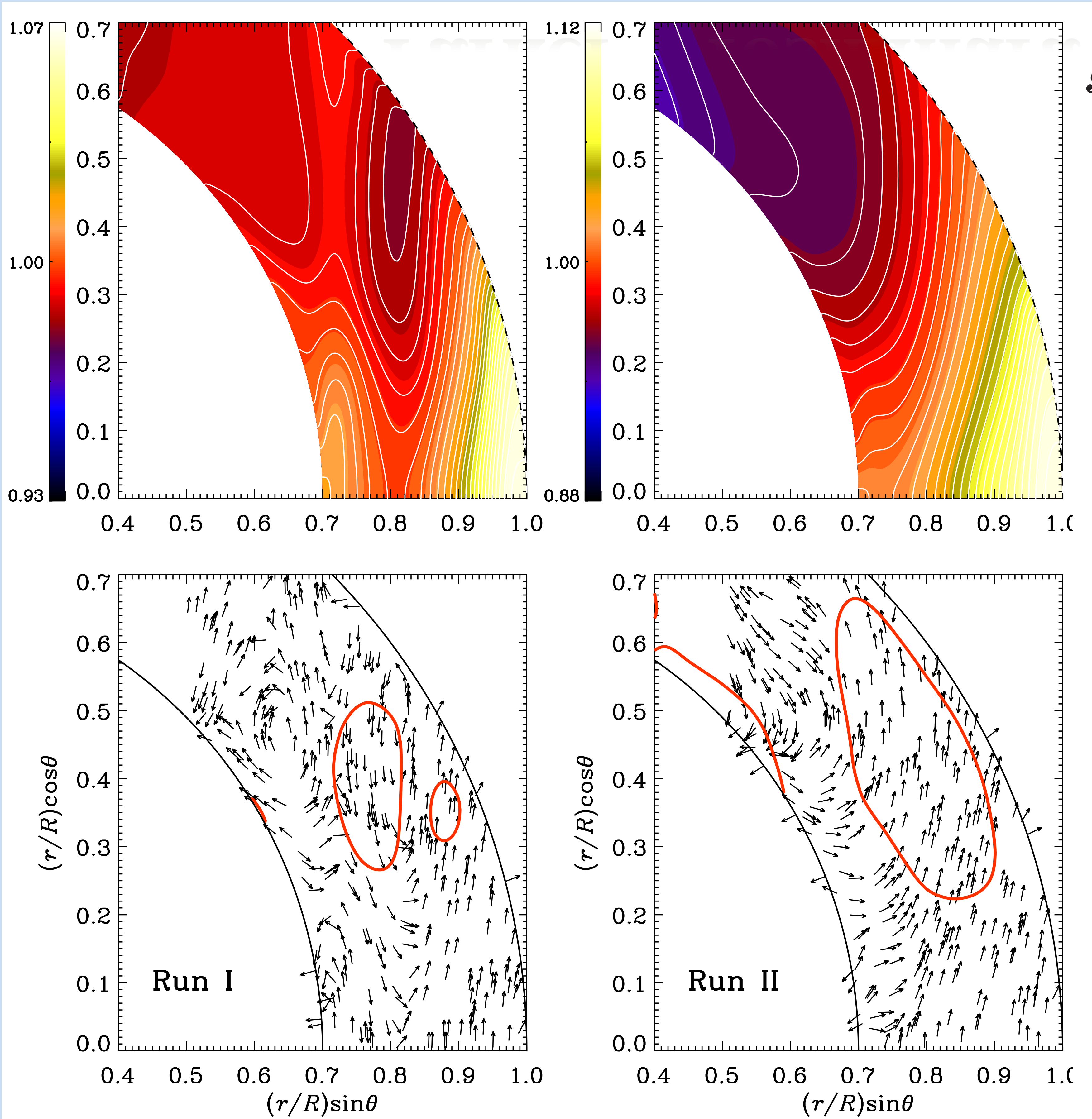

$$\boldsymbol{s}_{\rm mig}(r,\theta) = -\alpha\hat{\boldsymbol{e}}_\phi \times \boldsymbol{\nabla}\Omega,$$

Parker 1955
Yoshimura 1975

$$\alpha = \frac{\tau_{\rm c}}{3}\left(-\overline{\boldsymbol{\omega}\cdot\boldsymbol{u}} + \frac{\overline{\boldsymbol{j}\cdot\boldsymbol{b}}}{\overline{\rho}}\right)$$

Pouquet et al. 1976

Parker—Yoshimura—Rule

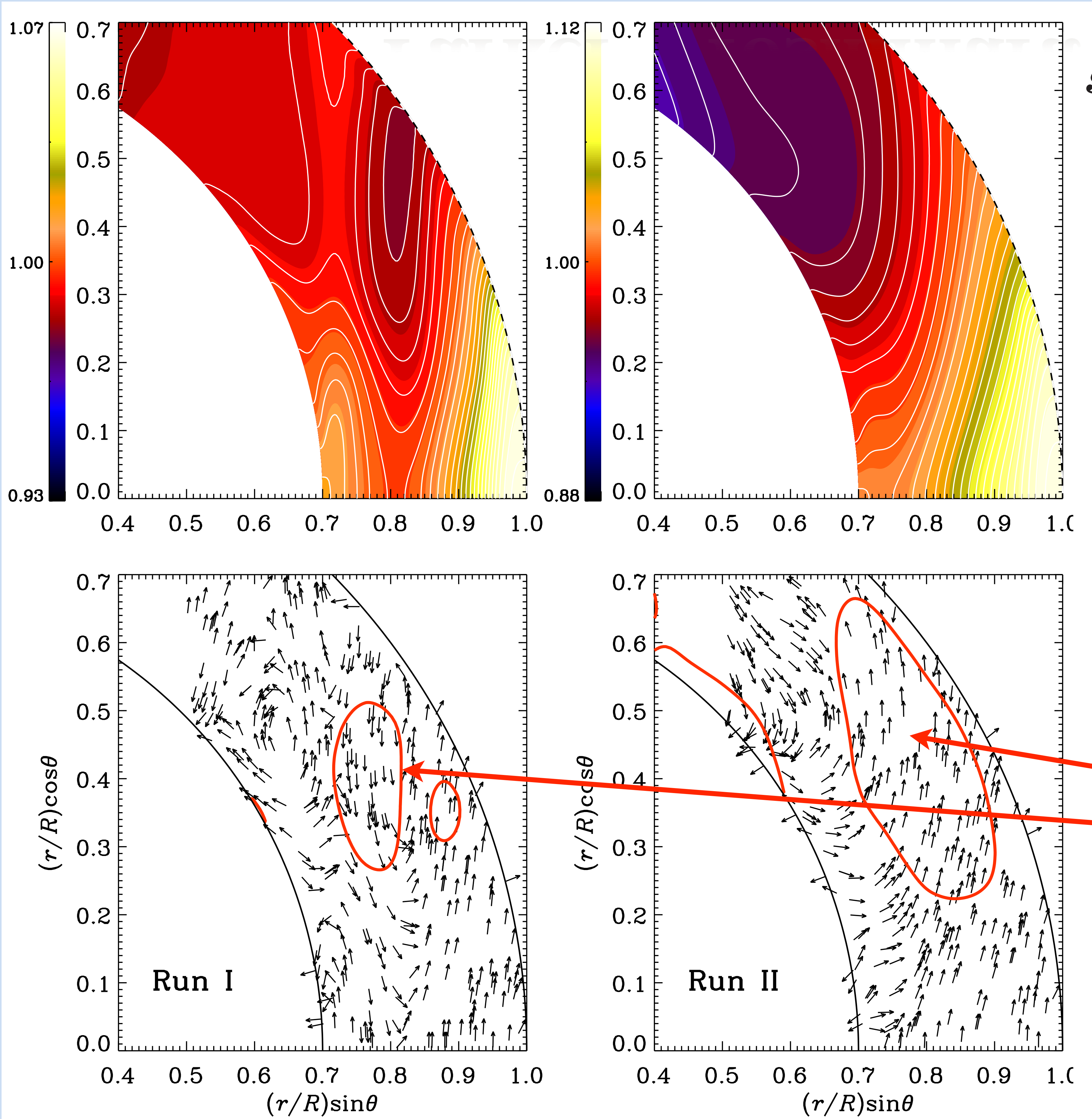

$$\boldsymbol{s}_{\rm mig}(r,\theta) = -\alpha \hat{\boldsymbol{e}}_\phi \times \boldsymbol{\nabla}\Omega,$$

Parker 1955

Yoshimura 1975

$$\alpha = \frac{\tau_c}{3}\left(-\overline{\boldsymbol{\omega}\cdot\boldsymbol{u}} + \frac{\overline{\boldsymbol{j}\cdot\boldsymbol{b}}}{\overline{\rho}}\right)$$

Pouquet et al. 1976

Strong toroidal field

Parker—Yoshimura—Rule

$$\boldsymbol{s}_{\rm mig}(r,\theta) = -\alpha \hat{\boldsymbol{e}}_\phi \times \boldsymbol{\nabla}\Omega,$$

Parker 1955

75

$$+ \frac{\overline{\boldsymbol{j}\cdot\boldsymbol{b}}}{\overline{\rho}}\Big)$$

1976

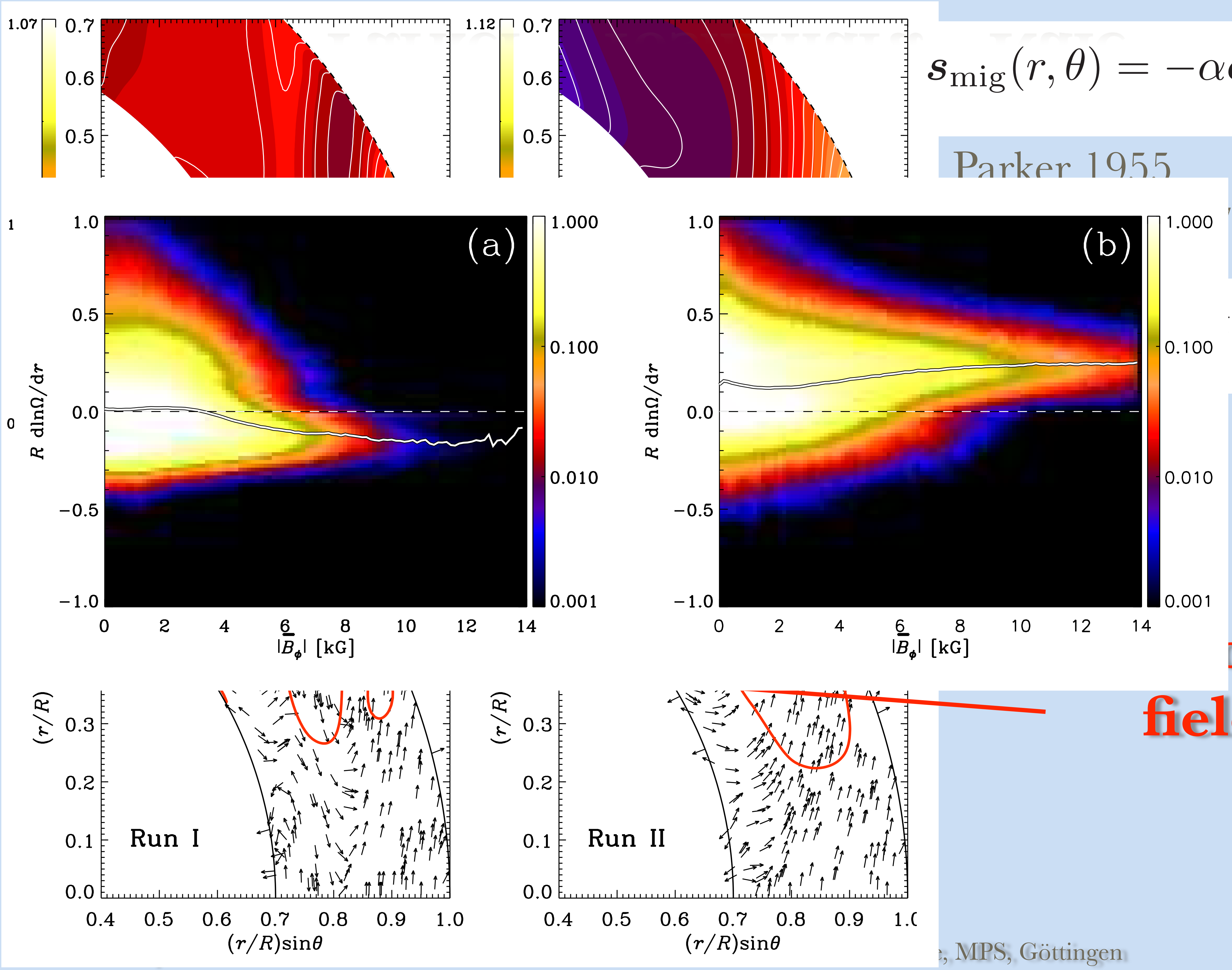

roidal
field

Differential rotation

Differential rotation

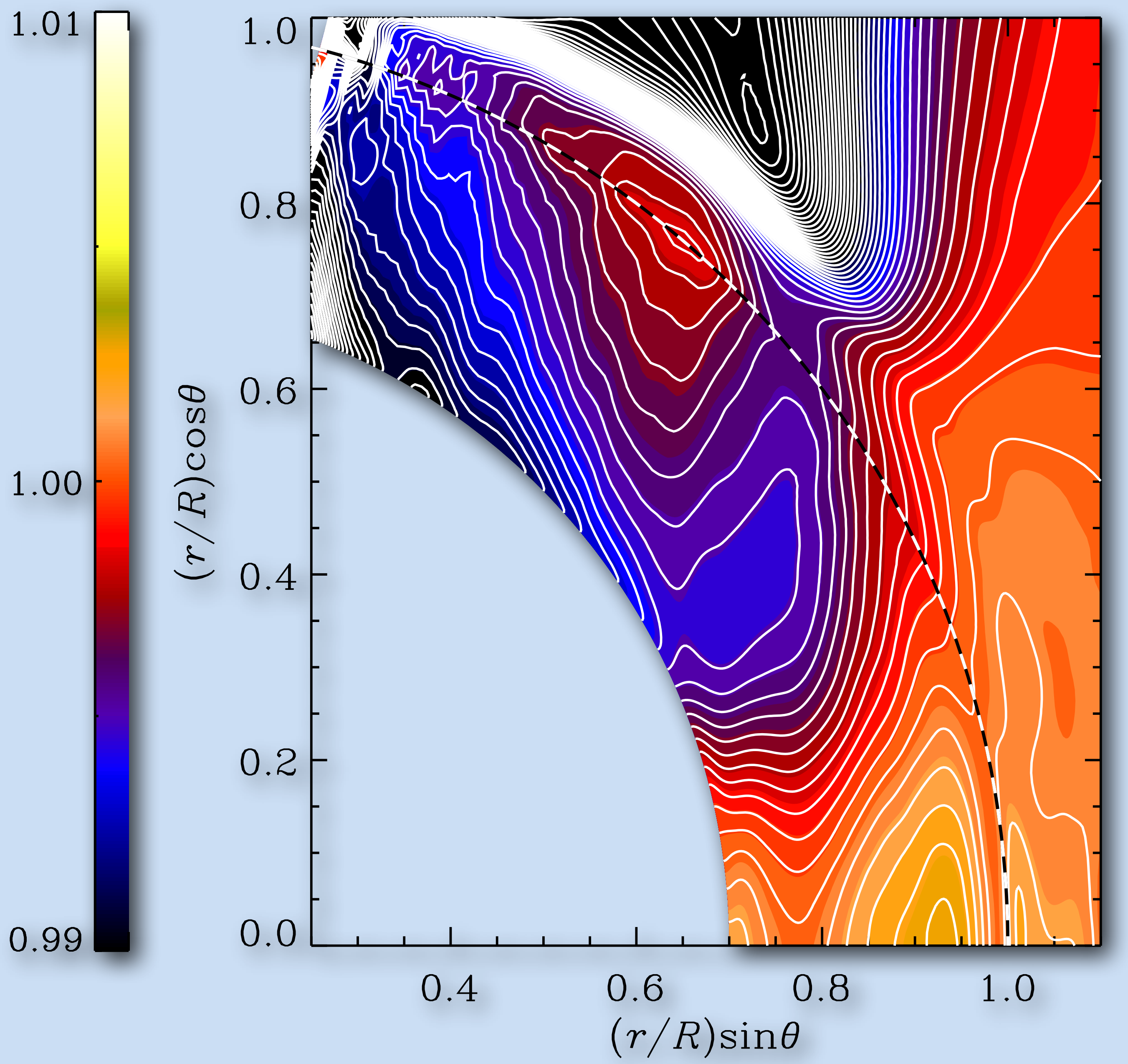

Differential rotation

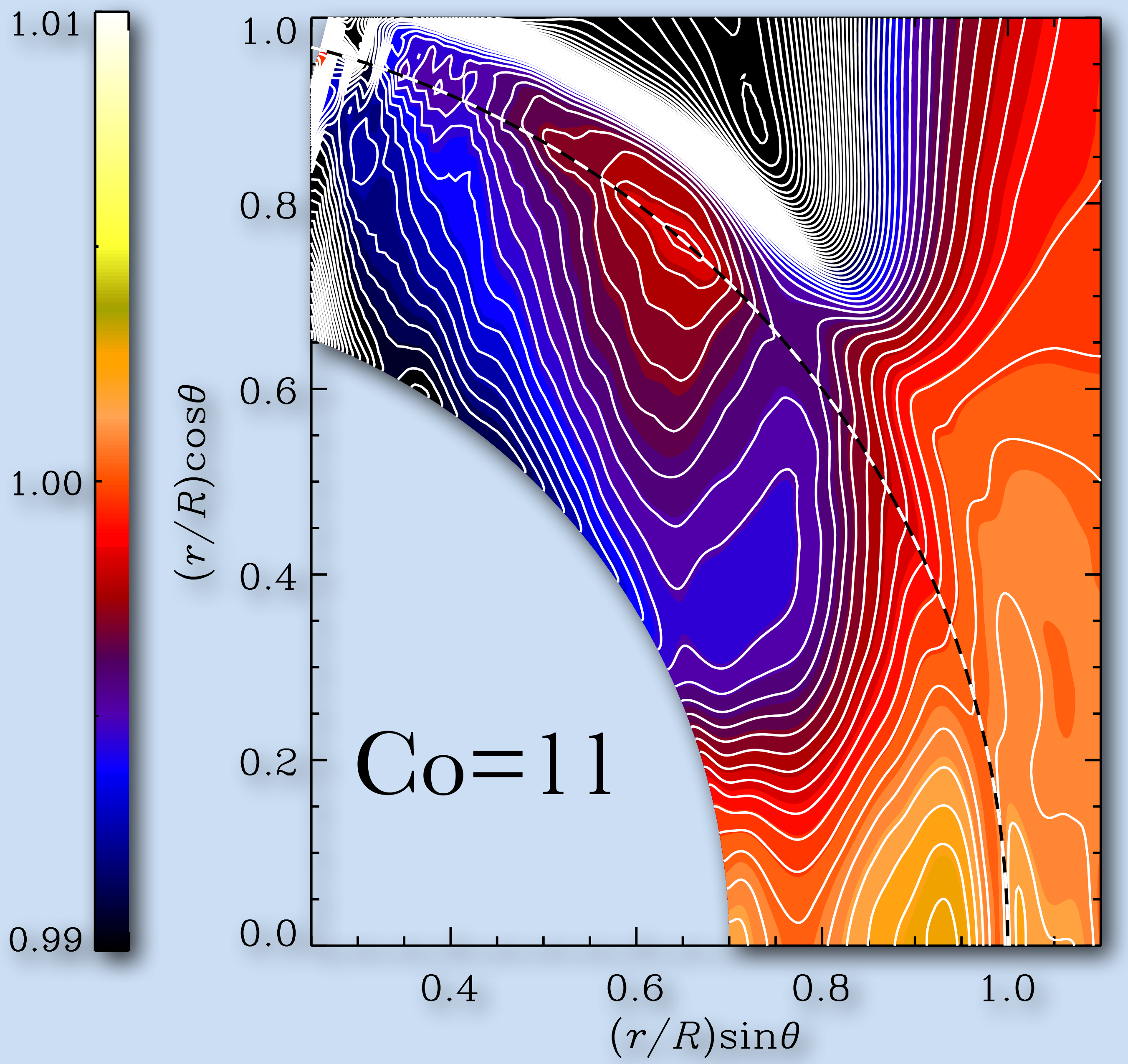

$$Co = \frac{2\Omega_0}{u_{rms}k_f} = \frac{2 \text{ Rotation rate}}{\text{Turnover time}}$$

Differential rotation

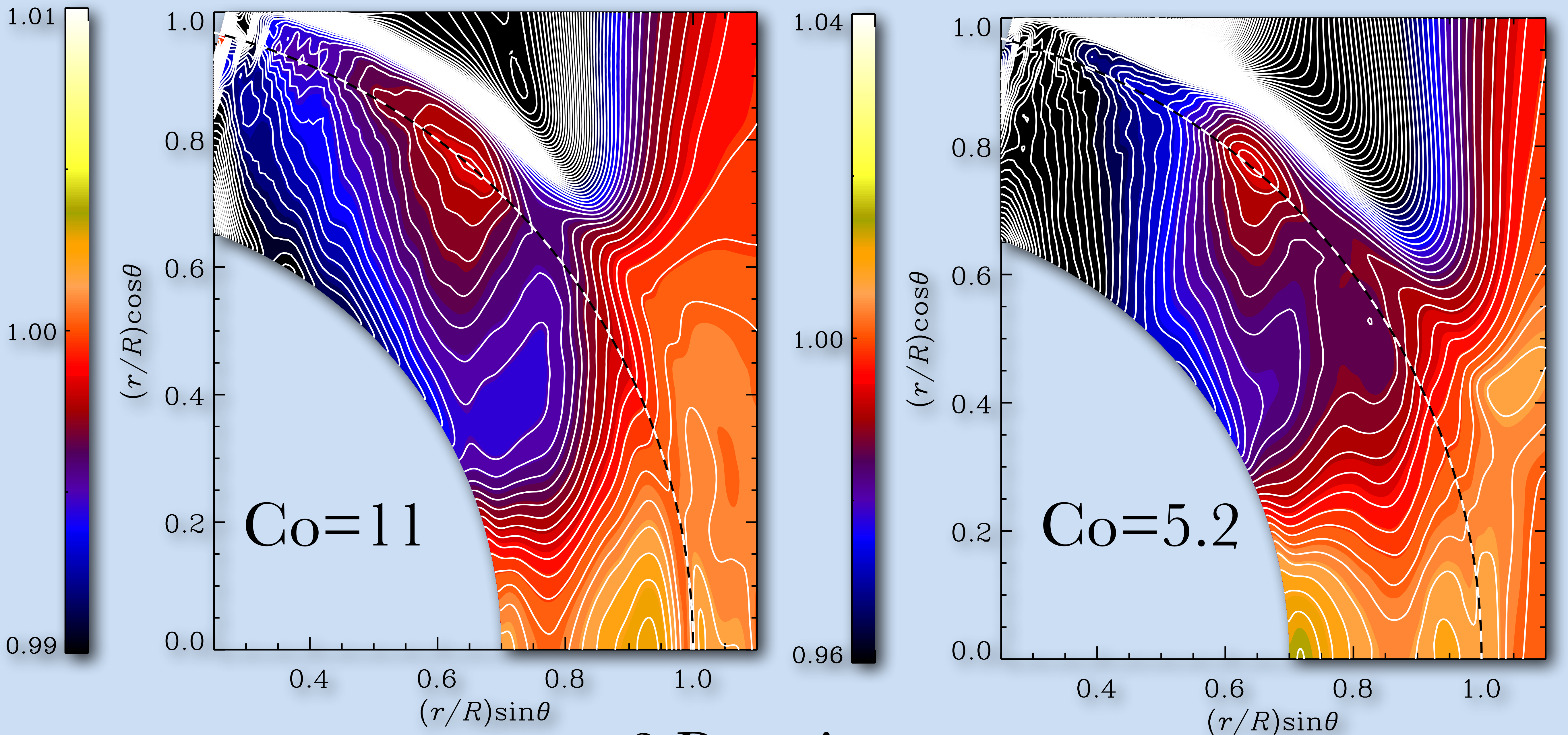

$$\mathrm{Co} = \frac{2\Omega_0}{u_{rms} k_f} = \frac{2 \text{ Rotation rate}}{\text{Turnover time}}$$

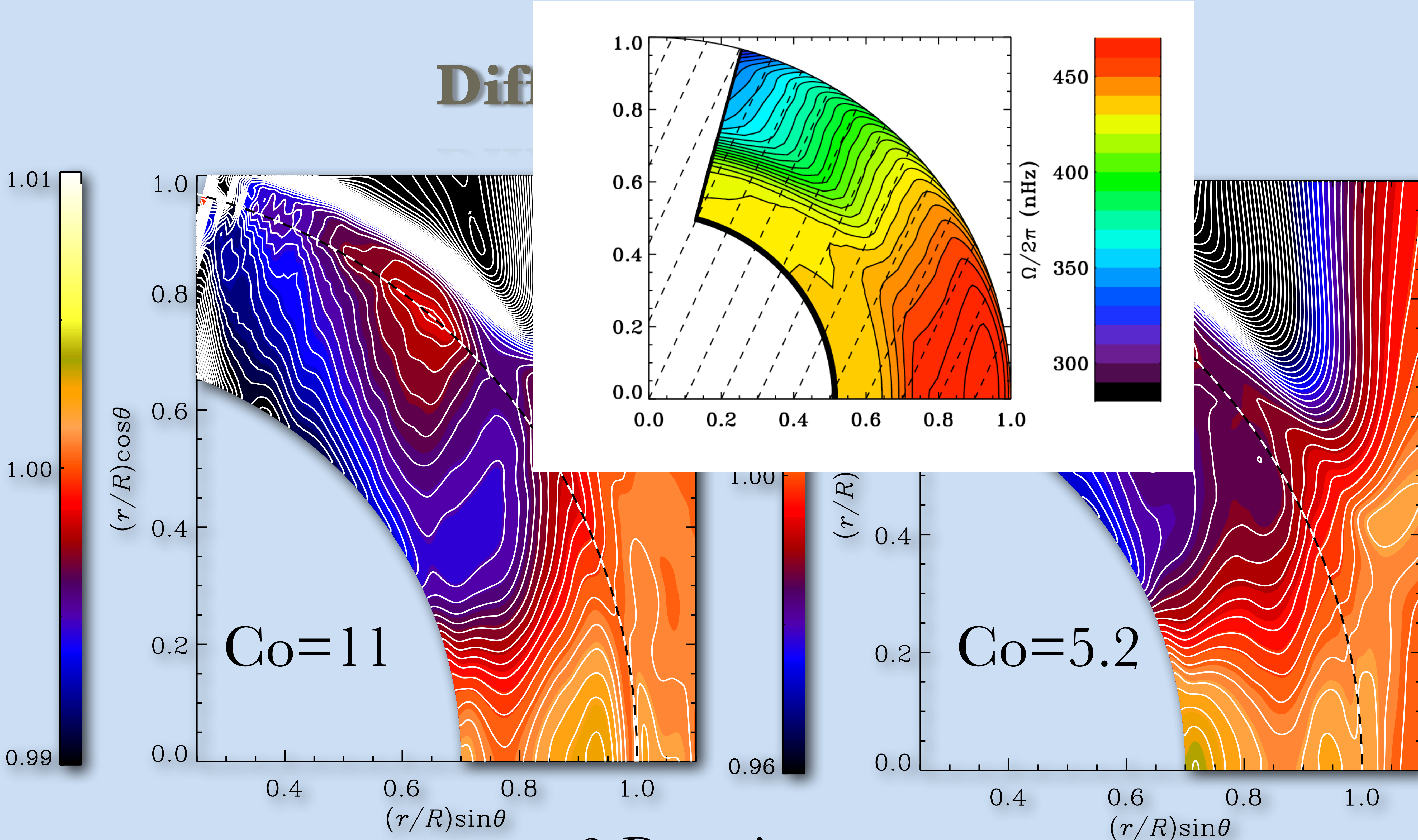

$$\mathrm{Co} = \frac{2\Omega_0}{u_{rms}k_f} = \frac{\text{2 Rotation rate}}{\text{Turnover time}}$$

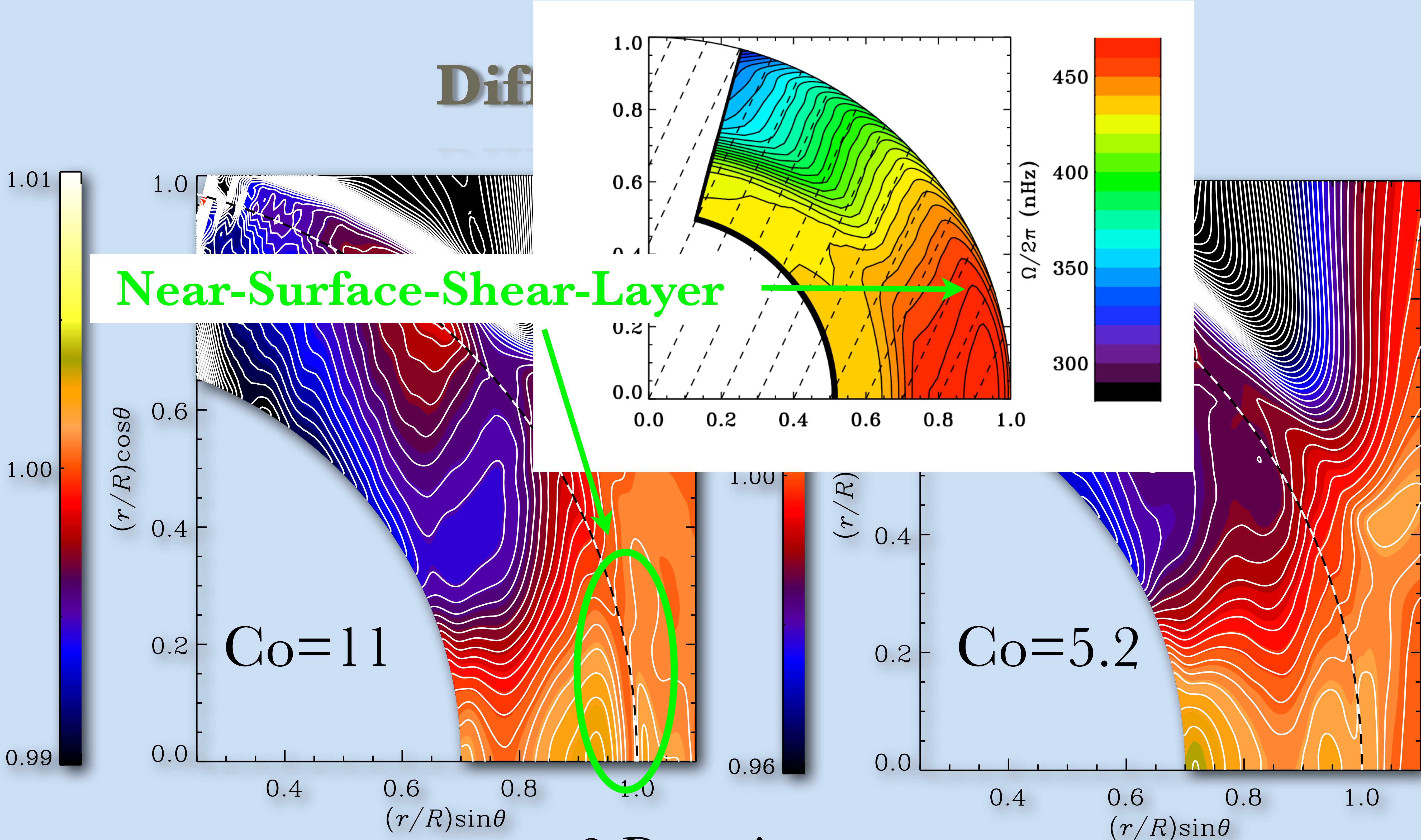

$$\mathrm{Co} = \frac{2\Omega_0}{u_{rms}k_f} = \frac{2\ \text{Rotation rate}}{\text{Turnover time}}$$

The Baroclinic Term

$$\frac{\partial \overline{\omega_\phi}}{\partial t} = r \sin\theta \frac{\partial \overline{\Omega}^2}{\partial z} + \left(\overline{\nabla T \times \nabla s}\right)_\phi + ...$$

The Baroclinic Term

Co=11

$$\frac{\partial \overline{\omega_\phi}}{\partial t} = r \sin\theta \frac{\partial \overline{\Omega}^2}{\partial z} + \left(\overline{\nabla T \times \nabla s}\right)_\phi + \ldots$$

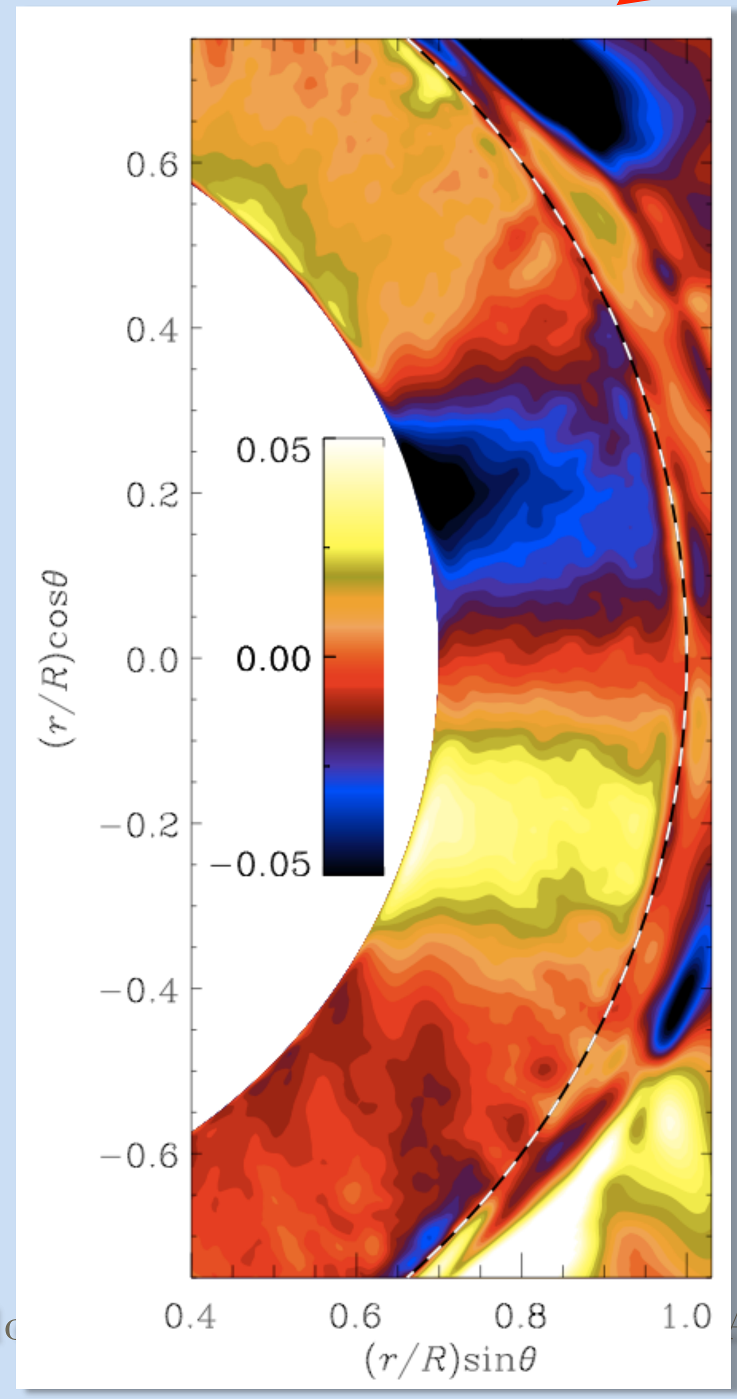

The Baroclinic Term

Co=11

$$\frac{\partial \overline{\omega_\phi}}{\partial t} = r \sin\theta \frac{\partial \overline{\Omega}^2}{\partial z} + \left(\overline{\nabla T \times \nabla s}\right)_\phi + \ldots$$

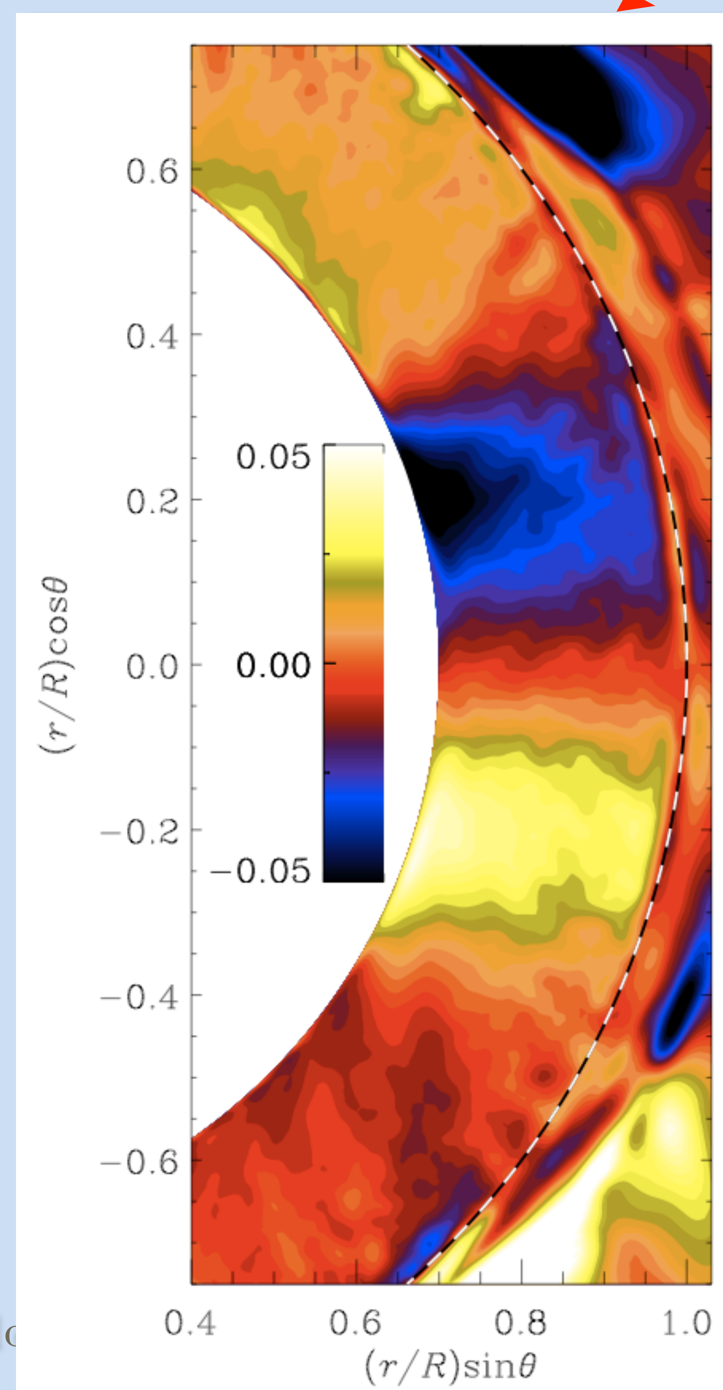

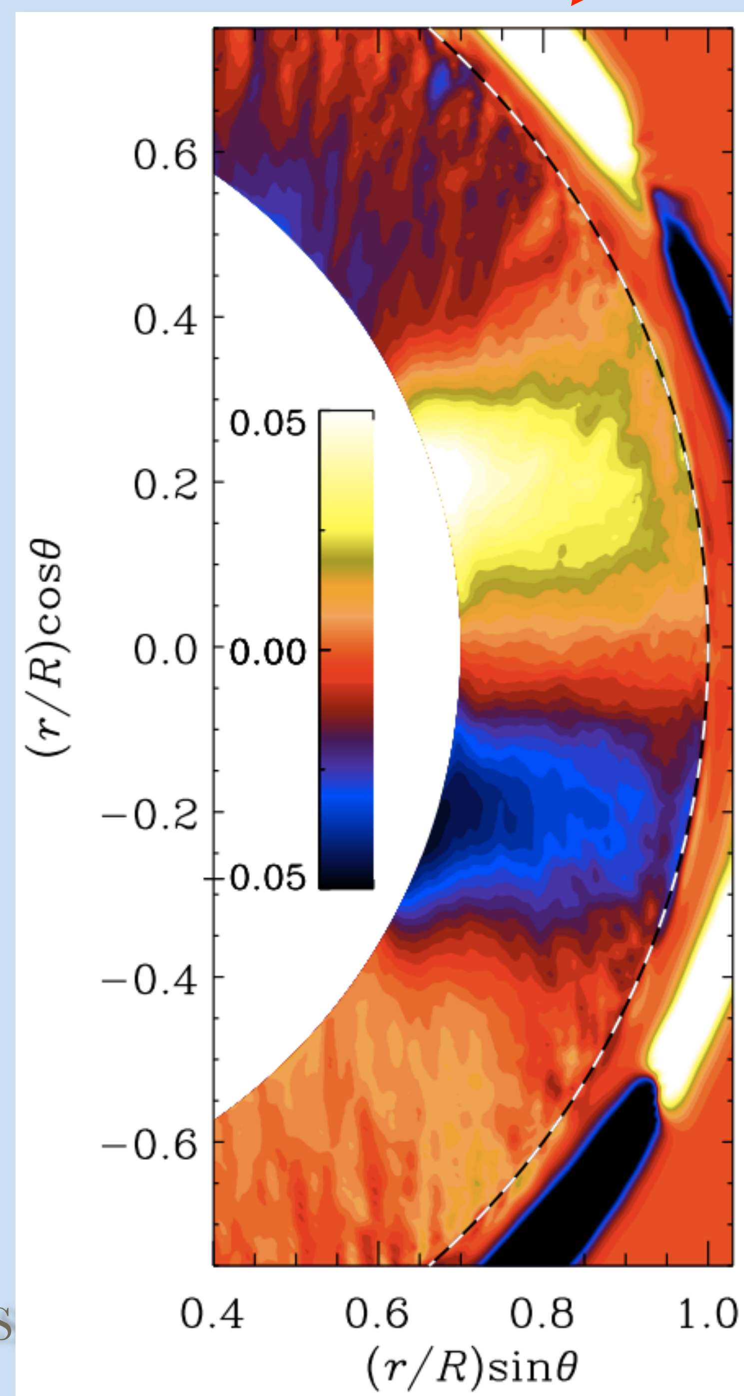

The Baroclinic Term

Co=11

$$\frac{\partial \overline{\omega_\phi}}{\partial t} = r\sin\theta \frac{\partial \overline{\Omega}^2}{\partial z} + \left(\overline{\nabla T \times \nabla s}\right)_\phi + \ldots$$

$$R\nabla_\theta \overline{s}/c_\mathrm{P}$$

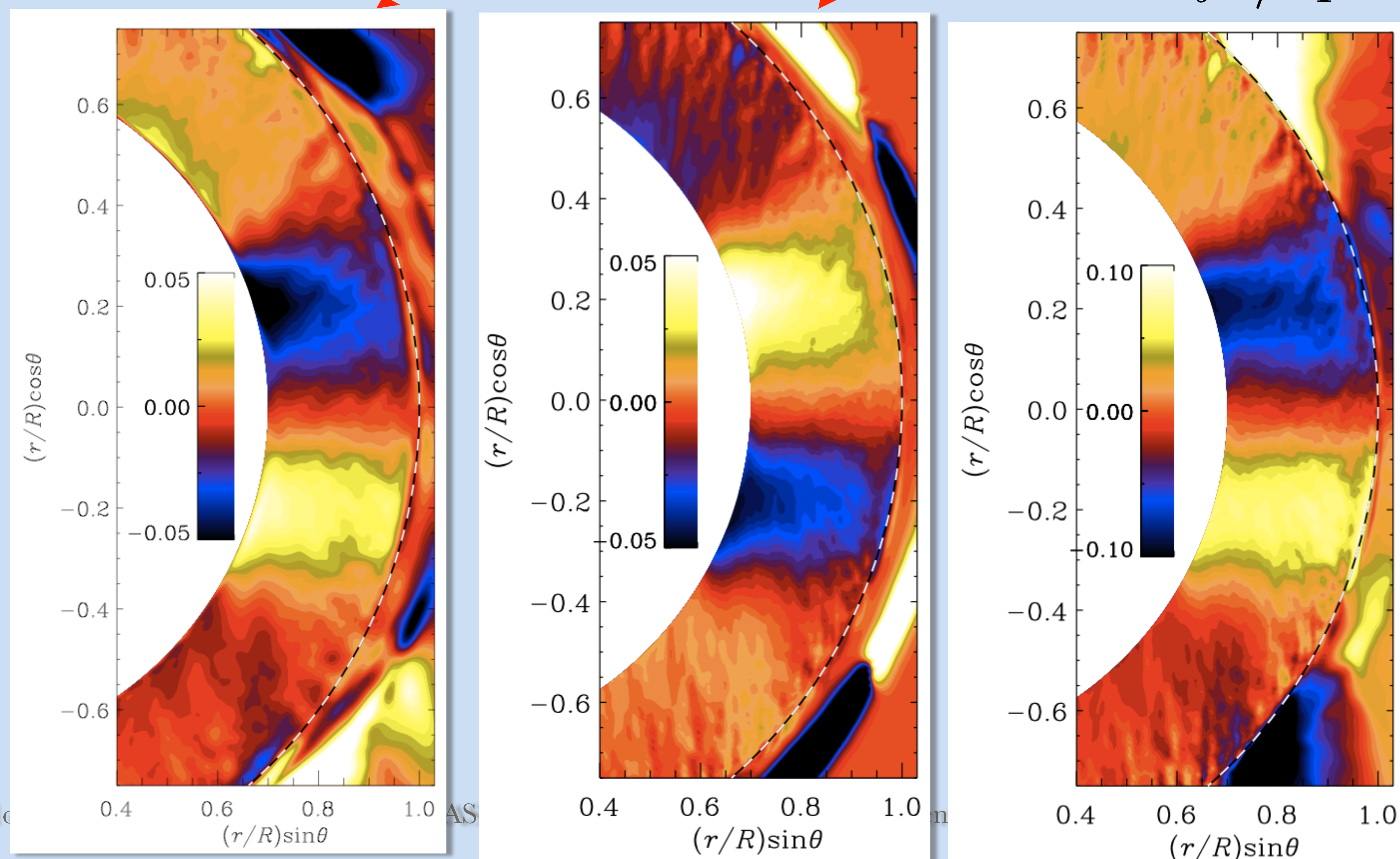

Turbulent heat conductivity

Turbulent heat conductivity

$$\overline{F_i} = -\chi_{ij}\overline{\rho}\overline{T}\nabla_j\overline{s}$$

Turbulent heat conductivity

$$\overline{F_i} = -\chi_{ij}\overline{\rho}\overline{T}\nabla_j\overline{s}$$

$$\overline{F_i} = c_{\mathrm{P}}\overline{\rho}\overline{u_i'T'},$$

Turbulent heat conductivity

$$\overline{F_i} = -\chi_{ij}\overline{\rho}\overline{T}\nabla_j\overline{s}$$

$$\overline{F_i} = c_{\mathrm{P}}\overline{\rho}\overline{u_i' T'},$$

$$\chi_{\theta r} \approx -c_{\mathrm{P}}\overline{u_\theta' T'} \Big/ \overline{T}\nabla_r\overline{s}.$$

Turbulent heat conductivity

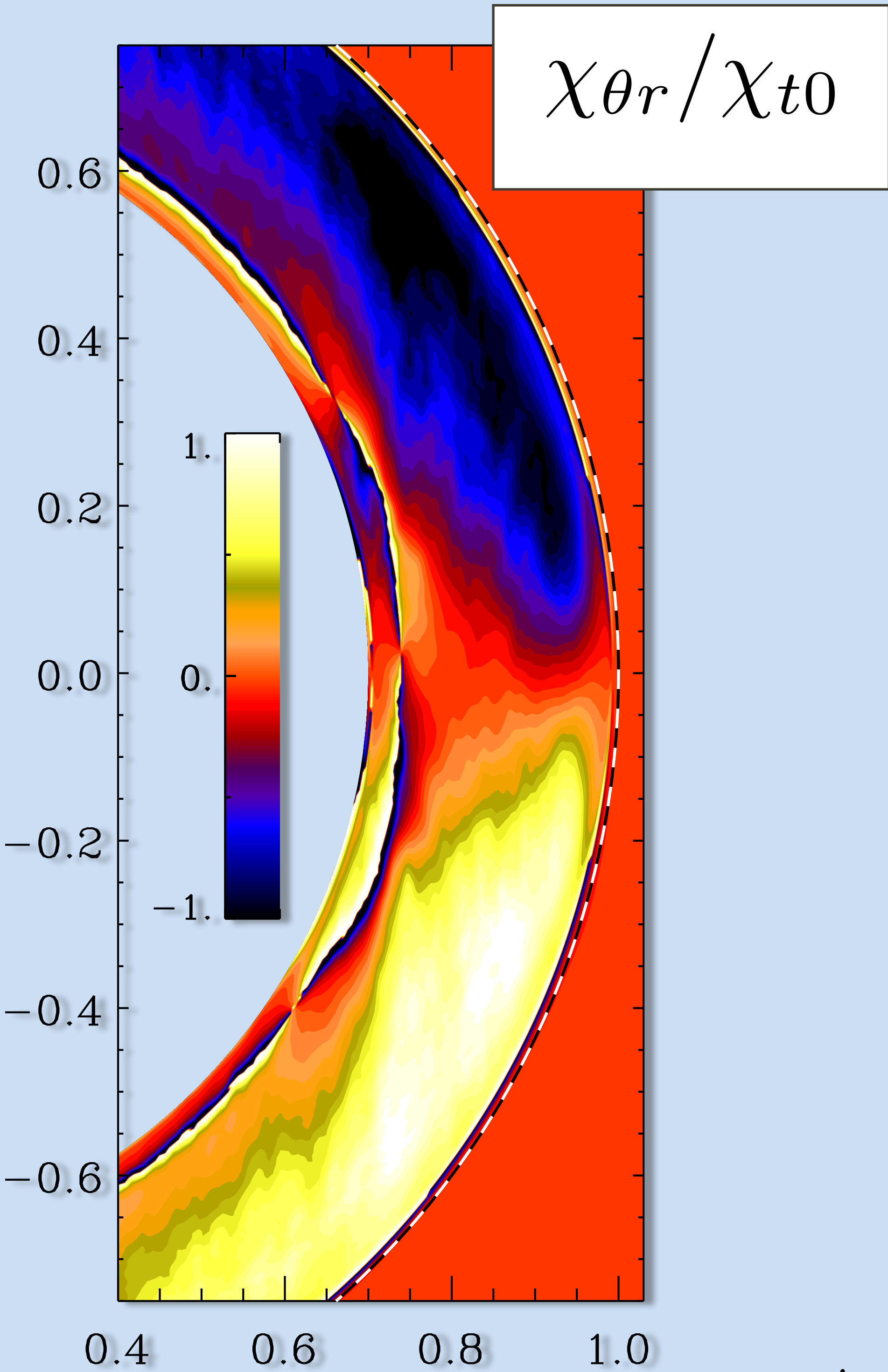

$$\overline{F_i} = -\chi_{ij}\overline{\rho}\overline{T}\nabla_j\overline{s}$$

$$\overline{F_i} = c_{\mathrm{P}}\overline{\rho}\overline{u_i' T'},$$

$$\chi_{t0} = u_{\mathrm{rms}}/3k_f$$

Co=11

$$\chi_{\theta r} \approx -c_{\mathrm{P}}\overline{u_\theta' T'} \Big/ \overline{T}\nabla_r\overline{s}.$$

Turbulent heat conductivity

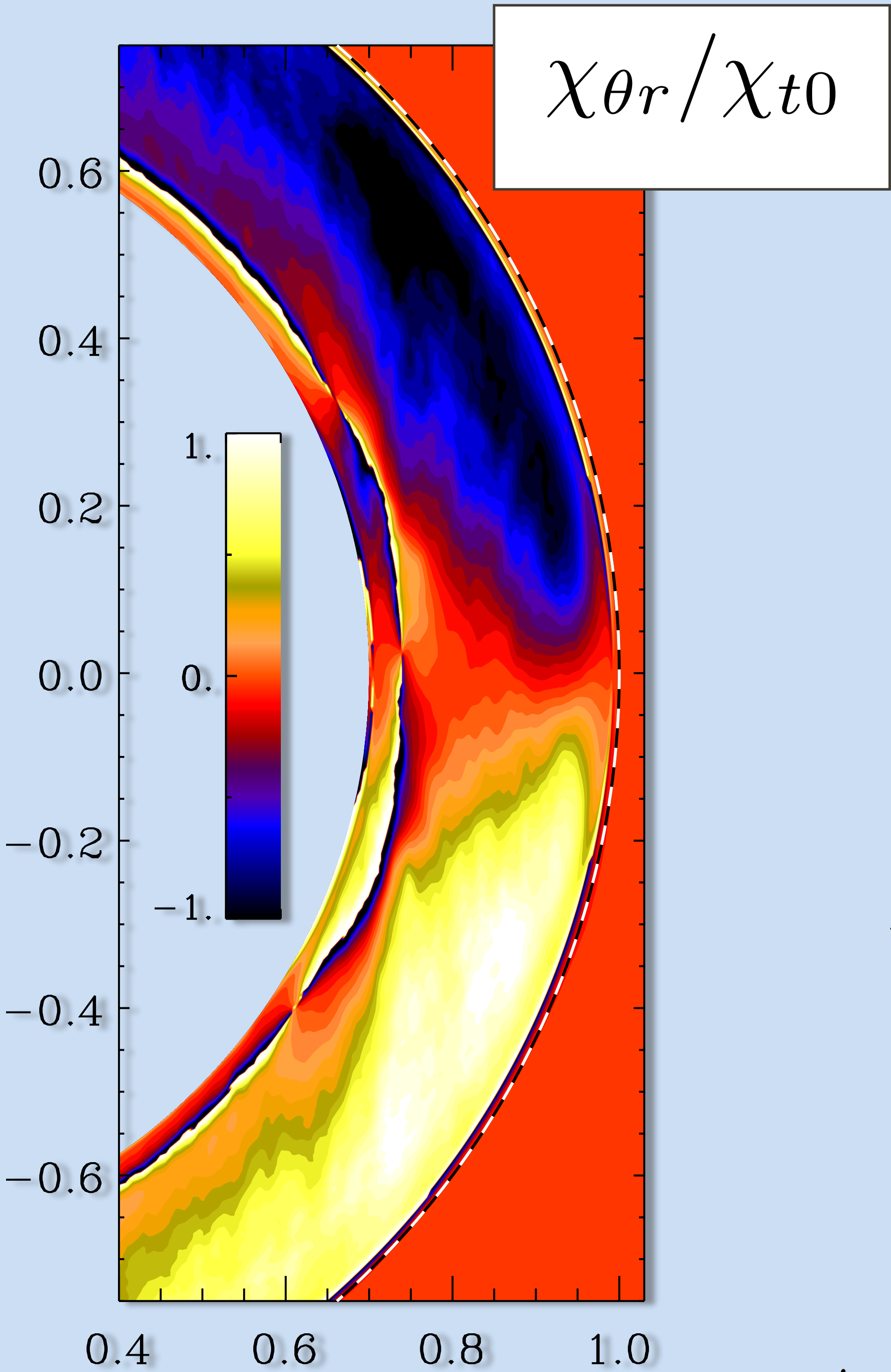

$$\overline{F}_i = -\chi_{ij}\overline{\rho}\,\overline{T}\nabla_j\overline{s}$$

$$\overline{F}_i = c_{\mathrm{P}}\overline{\rho}\,\overline{u_i'T'},$$

$$\chi_{t0} = u_{\mathrm{rms}}/3k_f$$

Co=11

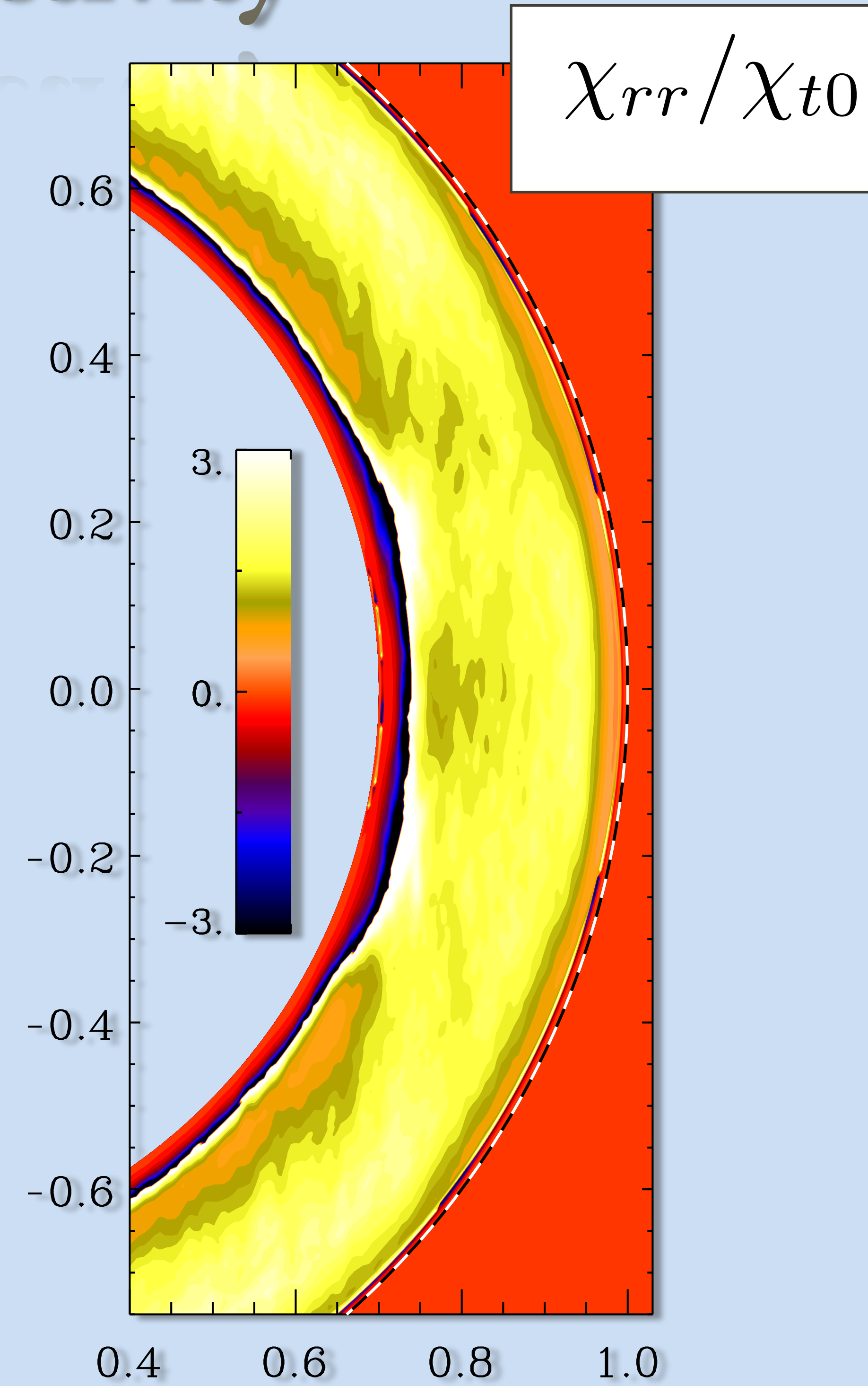

$$\chi_{\theta r} \approx -c_{\mathrm{P}}\overline{u_\theta'T'}\Big/\overline{T}\nabla_r\overline{s}.$$

$$\chi_{rr} \approx -c_{\mathrm{P}}\overline{u_r'T'}\big/\overline{T}\nabla_r\overline{s}.$$

Conclusions

Conclusions

- Migration of mean magnetic field can be entirely explained by an alpha-omega-dynamo wave

Conclusions

- Migration of mean magnetic field can be entirely explained by an alpha-omega-dynamo wave
- For equatorward mig. : alpha(+/-) x dOmega/dr(-/+)

Conclusions

- Migration of mean magnetic field can be entirely explained by an alpha-omega-dynamo wave
- For equatorward mig. : alpha(+/-) x dOmega/dr(-/+)
- A coronal envelope helps for Spoke-like rotation profile

Conclusions

- Migration of mean magnetic field can be entirely explained by an alpha-omega-dynamo wave
- For equatorward mig. : alpha(+/-) x dOmega/dr(-/+)
- A coronal envelope helps for Spoke-like rotation profile
- Self-consistent produced by a baroclinic term.

Conclusions

- Migration of mean magnetic field can be entirely explained by an alpha-omega-dynamo wave
- For equatorward mig. : alpha(+/-) x dOmega/dr(-/+)
- A coronal envelope helps for Spoke-like rotation profile
- Self-consistent produced by a baroclinic term.
- Near-surface shear layer is formed.

Conclusions

- Migration of mean magnetic field can be entirely explained by an alpha-omega-dynamo wave
- For equatorward mig. : alpha(+/-) x dOmega/dr(-/+)
- A coronal envelope helps for Spoke-like rotation profile
- Self-consistent produced by a baroclinic term.
- Near-surface shear layer is formed.
- Turbulent heat transport to the poles.

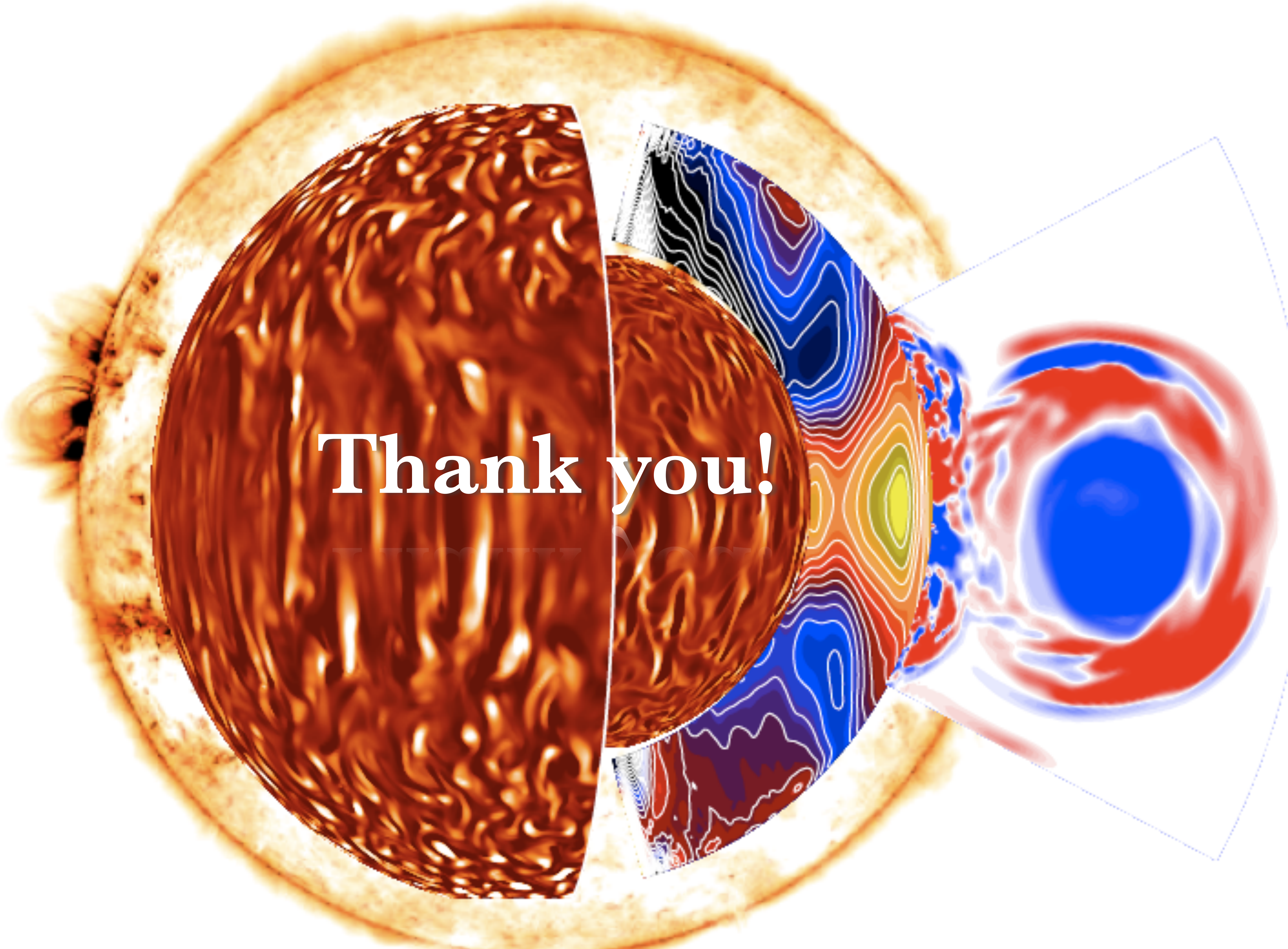
Thank you!